

## Supporting Information

### Thermodynamic and Transport Properties of H<sub>2</sub>O+NaCl from Polarizable Force Fields

Hao Jiang<sup>†</sup>, Zoltan Mester<sup>†</sup>, Othonas A. Moulton<sup>‡</sup>, Ioannis G. Economou<sup>‡</sup>,  
and Athanassios Z. Panagiotopoulos<sup>†</sup>

<sup>†</sup>*Department of Chemical and Biological Engineering, Princeton University., Princeton, New Jersey 08544, United States*

<sup>‡</sup>*Chemical Engineering Program, Texas A&M University at Qatar, P.O. Box 23874, Doha, Qatar*

Table 1: Force field parameters of BK3 water and ions models.

	Buckingham potential	charge $q(\text{e})$	Gaussian width $\sigma$ (Å)	polarizability $\alpha$ (Å $^3$ )	geometry
H <sub>2</sub> O	$A=322000 \text{ kJ/mol}$ $B=3.56 \text{ Å}^{-1}$ $C=3320 \text{ kJÅ}^6/\text{mol}$	$q_O=-1.168$ $q_H=0.584$	$\sigma_O=0.71$ $\sigma_H=0.4$	$\alpha_O=0.72$ $\alpha_H=0.36$	$d_{OH}=0.975\text{\AA}$ $\angle HOH=104.52^\circ$ $d_{OM}=0.2661\text{\AA}$
Na <sup>+</sup>	$A=8.5 \times 10^{12} \text{ kJ/mol}$ $B=15 \text{ Å}^{-1}$ $C=550 \text{ kJÅ}^6/\text{mol}$	$q_{Na} = 11$ $q_D = -10$	$\sigma_{Na}=0.65$ $\sigma_D=0.65$	$\alpha_{Na}=0.157$	
Cl <sup>-</sup>	$A=9.4 \times 10^5 \text{ kJ/mol}$ $B=3.1 \text{ Å}^{-1}$ $C=8000 \text{ kJÅ}^6/\text{mol}$	$q_{Cl} = -11$ $q_D = 10$	$\sigma_{Cl}=0.96$ $\sigma_D=0.96$	$\alpha_{Cl}=3.5$	

Table 2: Force field parameters of SWM4-NDP water and ions models.

	Lennard-Jones potential	charge $q(\text{e})$	polarizability $\alpha$ (Å $^3$ )	geometry
H <sub>2</sub> O	$\epsilon=0.883 \text{ kJ/mol}$ $\sigma=3.184 \text{ \AA}$	$q_O=1.71636$ $q_M=-1.11466$ $q_H=0.55733$ $q_D=-1.71636$	$\alpha_D=0.97825$	$d_{OH}=0.9572\text{\AA}$ $\angle HOH=104.52^\circ$ $d_{OM}=0.24034\text{\AA}$
Na <sup>+</sup>	$\epsilon=0.1316 \text{ kJ/mol}$ $\sigma=2.923 \text{ \AA}$	$q_{Na} = 1.688$ $q_D = -0.688$	$\alpha_{Na}=0.157$	
Cl <sup>-</sup>	$\epsilon=0.3008 \text{ kJ/mol}$ $\sigma=4.963 \text{ \AA}$	$q_{Cl} = 2.46$ $q_D = -3.46$	$\alpha_{Cl}=3.969$	

Table 3: Force field parameters of SPC/E+SD models

	Lennard-Jones potential	charge $q(\text{e})$	geometry
H <sub>2</sub> O	$\epsilon=0.65 \text{ kJ/mol}$ $\sigma=3.16 \text{ \AA}$	$q_O=-0.8476$ $q_M=0.4238$	$d_{OH}=1.0 \text{ \AA}$ $\angle HOH=109.47^\circ$
Na <sup>+</sup>	$\epsilon=0.5439 \text{ kJ/mol}$ $\sigma=2.35 \text{ \AA}$	$q_{Na} = 1.0$	
Cl <sup>-</sup>	$\epsilon=0.4184 \text{ kJ/mol}$ $\sigma=4.4 \text{ \AA}$	$q_{Cl} = -1.0$	

Table 4: Simulation results for relative permittivities  $\epsilon$  of BK3 and SPC/E water models at  $T = 298.15 \text{ K}$ ,  $373.15 \text{ K}$  and  $473.15 \text{ K}$ . Statistical uncertainties are given in parentheses in units of the last significant figure shown:  $80(2)$  means  $80 \pm 2$ .

$T$ (K)	$\epsilon$	
	BK3	SPC/E
298.15	80(2)	73(2)
373.15	56(2)	53(1)
473.15	34(1)	33(1)

Table 5: Simulation results for the liquid densities  $\rho (\text{kg/m}^3)$  of BK3 models at  $T = 298.15 \text{ K}$ ,  $373.15 \text{ K}$ ,  $473.15 \text{ K}$  and  $P = 100 \text{ bar}$ . Statistical uncertainties are given as in Table 4.

$m$ (mol/kg)	$\rho (\text{kg/m}^3)$		
	298.15 K	373.15 K	473.15 K
0.00	1002.4(3)	961.9(2)	863.5(2)
0.44	1019.6(3)	978.4(2)	882.8(4)
1.33	1053.5(3)	1010.6(5)	920.3(4)
2.22	1083.1(3)	1037.2(4)	948.3(3)
3.00	1107.2(5)	1060.0(4)	978.5(4)
4.22	1142.5(6)	1093.6(3)	1008.4(4)

Table 6: Simulation results for the liquid densities  $\rho (\text{kg/m}^3)$  of SPC/E+SD models at  $T = 298.15 \text{ K}$ ,  $373.15 \text{ K}$ ,  $473.15 \text{ K}$  and  $P = 100 \text{ bar}$ . Statistical uncertainties are given as in Table 4.

$m$ (mol/kg)	$\rho (\text{kg/m}^3)$		
	298.15 K	373.15 K	473.15 K
0.00	1001.2(7)	949.1(4)	841(1)
1.00	1040.9(3)	988.4(4)	886.4(6)
2.00	1076.8(3)	1022.6(5)	923.6(6)
3.00	1107.8(5)	1053.1(5)	955.3(6)
4.00	1135.3(3)	1078.2(4)	982.4(5)

Table 7: Simulation results for the electrolyte chemical potential  $\mu$  (kJ/mol) and mean ionic activity coefficients  $\gamma$  of BK3 models at  $T = 298.15$  K, 373.15 K and 473.15 K. Statistical uncertainties are given as in Table 4.

$m$ (mol/kg)	298.15 K, 1 bar		373.15 K, 1 bar		473.15 K, 15.5 bar	
	$\mu$ (kJ/mol)	$\ln\gamma$	$\mu$ (kJ/mol)	$\ln\gamma$	$\mu$ (kJ/mol)	$\ln\gamma$
0.11	-409.2(3)	-0.26(1)	-405.6(3)	-0.32(2)	-399.3(4)	-0.46(2)
0.44	-402.8(3)	-0.35(8)	-397.5(3)	-0.39(7)	-389.6(4)	-0.61(7)
1.33	-397.4(3)	-0.41(8)	-391.3(4)	-0.52(7)	-383.2(4)	-0.93(6)
2.22	-394.8(3)	-0.37(8)	-388.0(3)	-0.47(7)	-379.8(4)	-0.98(7)
3.00	-393.1(3)	-0.32(8)	-386.3(3)	-0.51(7)	-378.4(4)	-1.10(7)
4.22	-391.1(3)	-0.26(8)	-384.3(3)	-0.51(7)	-376.5(4)	-1.20(6)

Table 8: Simulation results for the electrolyte chemical potential  $\mu$  (kJ/mol) and mean ionic activity coefficients  $\gamma$  of SPC/E+SD models at  $T = 298.15$  K, 373.15 K and 473.15 K. Statistical uncertainties are given as in Table 4.

$m$ (mol/kg)	298.15 K, 1 bar <sup>†</sup>		373.15 K, 1bar		473.15 K, 15.5 bar	
	$\mu$ (kJ/mol)	$\ln\gamma$	$\mu$ (kJ/mol)	$\ln\gamma$	(mol/kg)	$\mu$ (kJ/mol)
0.011	-403.1(2)	-0.138(6)	-400.7(2)	-0.141(4)	-394.0(2)	-0.200(9)
0.06	-395.6(2)	-0.24(5)	—	—	—	—
0.11	—	—	-387.6(2)	-0.33(4)	-378.5(2)	-0.54(3)
0.56	-384.5(2)	-0.31(4)	-378.1(2)	-0.41(4)	-367.6(2)	-0.76(3)
1.00	-381.8(2)	-0.34(4)	-374.0(2)	-0.34(4)	-363.6(2)	-0.85(3)
2.00	-377.7(2)	-0.21(5)	—	—	—	—
3.00	-375.1(2)	-0.10(5)	-367.5(2)	-0.39(4)	-357.0(2)	-1.10(3)
4.00	-373.3(2)	-0.03(5)	—	—	—	—
5.00	-371.7(2)	0.08(5)	-363.9(2)	-0.34(4)	-354.2(2)	-1.25(3)
6.00	-370.5(2)	0.14(5)	-362.9(2)	-0.34(4)	-353.2(2)	-1.32(3)

<sup>†</sup> Data are from Z. Mester and A. Z. Panagiotopoulos, J. Chem. Phys. 142, 044507-10 (2015).

Table 9: Henry's law standard chemical potential  $\mu^\dagger$  (kJ/mol) of BK3 and SPC/E+SD models at  $T = 298.15$  K, 373.15 K and 473.15 K. Statistical uncertainties are given as in Table 4.

T(K)	P(bar)	$\mu_{\text{BK3}}^\dagger$ (kJ/mol)	$\mu_{\text{SPC/E+SD}}^\dagger$ (kJ/mol)
298.15 K	1.0 bar	-397.0(3)	-380.1(2)
373.15 K	1.0 bar	-389.9(3)	-371.9(2)
473.15 K	15.5 bar	-378.3(4)	-357.0(2)

Table 10: Simulation results for the crystal chemical potential  $\mu$  (kJ/mol), crystal density  $\rho$  (kg/m<sup>3</sup>) and salt solubilities of BK3 models at  $T = 298.15$  K, 373.15 K and 473.15 K. Statistical uncertainties are given as in Table 4.

$T$ (K)	$\mu$ (kJ/mol)	$\rho$ (kg/m <sup>3</sup> )	solubility (mol/kg)
298.15	-399.0(2)	2115.8(4)	0.99(5)
373.15	-390.6(2)	2097.8(3)	1.48(6)
473.15	-379.4(3)	2073.0(4)	2.5(1)

Table 11: Simulation results for the crystal chemical potential  $\mu$  (kJ/mol), crystal density  $\rho$  (kg/m<sup>3</sup>) and salt solubilities of SD models at  $T = 298.15$  K, 373.15 K and 473.15 K. Data are from reference [66]. Statistical uncertainties are given as in Table 4.

$T$ (K)	$\mu$ (kJ/mol)	$\rho$ (kg/m <sup>3</sup> )	solubility (mol/kg)
298.15	-384.019(2)	1932.4(1)	0.63(1)
373.15	-376.241(2)	1916.4(1)	0.73(1)
473.15	-365.331(2)	1894.7(1)	0.78(2)

Table 12: Simulation results for vapor pressures  $P^{sat}$  (bar) of BK3 models at  $T = 373.15$  K and 473.15 K. Statistical uncertainties are given as in Table 4.

$m$ (mol/kg)	$P^{sat}$ (bar)	
	373.15 K	473.15 K
0.00	1.12(4) <sup>†</sup>	18.6(4) <sup>†</sup>
0.43	1.13(4)	18.4(5)
1.30	1.05(4)	18.1(5)
2.17	0.99(5)	17.2(6)
3.03	0.98(4)	16.6(6)
4.33	0.93(5)	16.3(5)
4.99	0.94(7)	16.1(5)

<sup>†</sup>Data are obtained from extrapolating vapor pressure of solution to zero salt concentration.

Table 13: Fitting parameters in Eq.12 for BK3 models at  $T = 373.15$  K and 473.15 K.

Parameter	373.15 K	473.15 K
A	0.604	0.894
B	1.361	1.486
b	-0.216	-0.458
C	0.070	0.099
D	-0.007	-0.008

Table 14: Simulation results for vapor pressures  $P^{sat}$  (bar) of AH/SWM4-NDP models at  $T = 373.15$  K. Statistical uncertainties are given as in Table 4.

$m$ (mol/kg)	$P^{sat}$ (bar)
0.00	3.1(1)
1.00	3.5(1)
2.00	3.7(1)
3.00	4.0(1)

Table 15: Simulation results for vapor-liquid interfacial tensions  $\sigma$  (mN/m) of BK3 models at  $T = 298.15$  K, 373.15 K and 473.15 K. Statistical uncertainties are given as in Table 4.

$m$ (mol/kg)	$\sigma$ (mN/m)		
	298.15 K	373.15 K	473.15 K
0.44	67.9(8)	54.5(8)	33.3(8)
1.33	70(1)	56.8(7)	36.6(6)
2.22	70.5(8)	58.1(6)	39.2(6)
3.00	72(1)	60.3(6)	40.9(6)
4.33	74.0(9)	60.9(7)	42.8(8)
5.00	76.1(7)	62.5(7)	44.2(6)

Table 16: Simulation results for shear viscosities  $\eta$  (cP) of BK3 models at  $T = 298.15$  K, 373.15 K and 473.15 K. Statistical uncertainties are given as in Table 4.

$m$ (mol/kg)	$\eta$ (cP)		
	298.15 K	373.15 K	473.15 K
0.00	1.00(4)	0.299(8)	0.133(3)
0.44	1.05(1)	0.31(1)	0.145(4)
1.00	1.12(5)	0.33(1)	0.154(2)
2.00	1.29(4)	0.39(1)	0.179(6)
3.00	1.41(3)	0.44(1)	0.199(5)
4.00	1.57(9)	0.51(2)	0.219(4)
6.00	2.4(1)	0.61(2)	0.228(5)

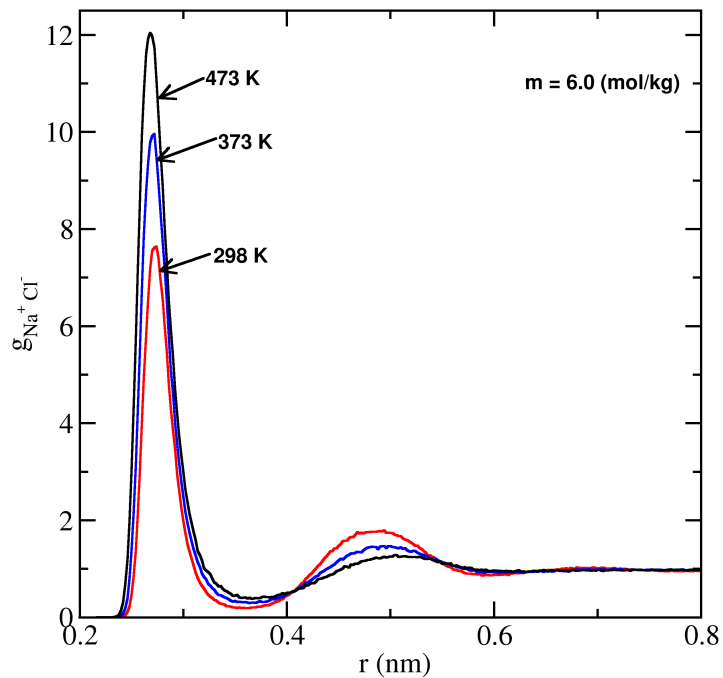


Figure 1: Radial distribution functions between  $\text{Na}^+$  and  $\text{Cl}^-$  of binary  $\text{H}_2\text{O} + \text{NaCl}$  mixture with BK3 models at  $m = 6.0$ , and  $T = 298.15$  K,  $373.15$  K and  $473.15$  K.

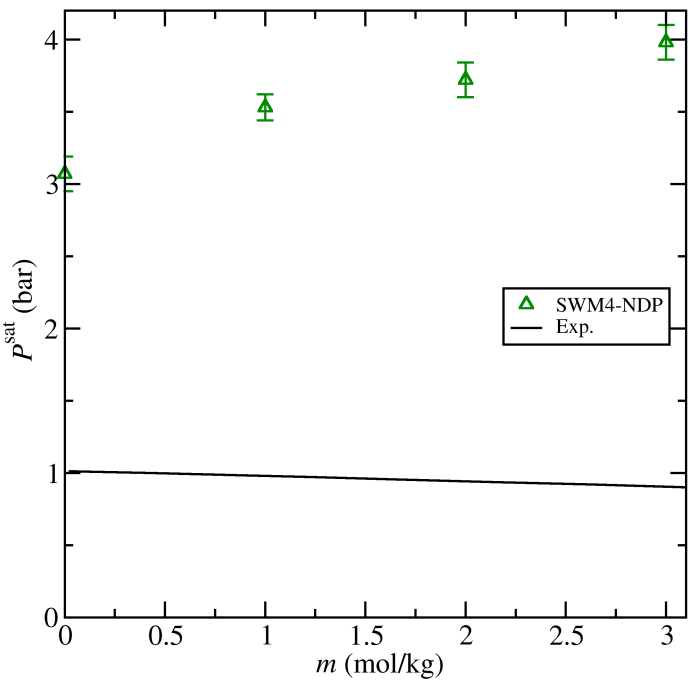


Figure 2: Vapor pressures  $P^{\text{sat}}$  (bar) for AH/SWM4-NDP models of the system  $\text{H}_2\text{O} + \text{NaCl}$  at  $T = 373.15 \text{ K}$  *versus* NaCl molality,  $m$ , in mol NaCl / kg of  $\text{H}_2\text{O}$ . Symbols are simulation results, and solid line is experimental data (S. L. Phillips, A. Igbene, J. A. Fair, H. Ozbek, and H. Tavana., A Technical Databook for Geothermal Energy Utilization).